

ICASE

COMPACT DIFFERENCE SCHEMES FOR MIXED
INITIAL BOUNDARY VALUE PROBLEMS - I

NASA-CR-175810
19850019198

Richard B. Philips

and

Milton E. Rose

LIBRARY COPY

DEC 21 1990

LANGLEY RESEARCH CENTER
LIBRARY NASA, HAMPTON, VA.

Report No. 81-4

January 21, 1981

INSTITUTE FOR COMPUTER APPLICATIONS IN SCIENCE AND ENGINEERING
NASA Langley Research Center, Hampton, Virginia

Operated by the

UNIVERSITIES SPACE



RESEARCH ASSOCIATION



NF00470

COMPACT DIFFERENCE SCHEMES
FOR MIXED INITIAL BOUNDARY VALUE PROBLEMS - I

Richard B. Philips
*Institute for Computer Applications in Science and Engineering
and Old Dominion University*

and

Milton E. Rose
Institute for Computer Applications in Science and Engineering

ABSTRACT

Compact finite difference schemes for hyperbolic and convection-diffusion equations are presented and their relationships to box schemes are described. A simple modification of the mesh ratio $\Delta t/\Delta x$ is shown to make a previously described non-dissipative scheme for the hyperbolic problem dissipative. The dissipative scheme for the convective-diffusion equation is formally second order accurate for all values of the local cell Reynolds number. Applications to nonlinear problems are described.

This report was prepared as a result of work performed under NASA Contracts No. NAS1-14472 and NAS1-15810 at ICASE, NASA Langley Research Center, Hampton, VA 23665.

N85-72820

Introduction

This paper describes implicit finite difference schemes for two closely related classes of mixed initial-boundary value problems in one space dimension.

Part I treats the hyperbolic problem:

$$(1a) \quad U_t + AU_x = 0, \quad 0 < x < 1, \quad 0 < t < T$$

with the initial and boundary conditions

$$U = U^0, \quad t = 0$$

$$(1b) \quad B_0 U = g_0, \quad x = 0$$

$$B_1 U = g_1, \quad x = 1.$$

Here A is a nonsingular $(r \times r)$ matrix with k positive and ℓ negative real eigenvalues while B_0 is $(k \times r)$ of rank k and B_1 is $(\ell \times r)$ of rank ℓ , $k + \ell = r$. The boundary conditions are assumed to be dissipative, i.e. for every vector satisfying the homogeneous boundary conditions then $(-1)^{x+1} U'AU \geq 0$ for $x = 0, 1$.

Note that the differential equation in (1) is the nonconservative form of the system $U_t + F_x(U) = 0$ where $A = \text{grad} F$.

Part II treats the scalar convective-diffusion equation ($v > 0$)

$$(2) \quad u_t + au_x - v u_{xx} = 0, \quad 0 < x < 1, \quad 0 < t < T,$$

which we write as the system

$$(2a) \quad u_t + au_x - v v_x = 0$$

$$u_x - v = 0;$$

with $W = (u, v)'$, initial and boundary conditions are

$$u = u^0, \quad t = 0$$

$$(2b) \quad B_0 W = g_0, \quad x = 0$$

$$B_1 W = g_1, \quad x = 1,$$

where B_0, B_1 are both (1×2) . We also assume that homogeneous boundary conditions result in the inequalities $(-1)^{x+1}(au - vv)u \geq 0$, $x = 0, 1$.

We are interested in demonstrating the following:

a) the dissipative implicit finite difference schemes described below allow the related nonlinear conservation forms of (1) and (2) to be treated in their nonconservation forms; numerical evidence for this assertion is provided below.

b) for the linear hyperbolic equation dissipation can be restricted to affect amplitude modulation while phase errors will be affected only by the CFL number; it is thus possible to control pre or post oscillations at a discontinuity by the choice of the mesh ratio $\lambda = \Delta t / \Delta x$.

c) for the convective-diffusion equation the scheme is second order accurate for all values of the "local cell Reynolds number" $(|a| \Delta x) / (2\nu)$.

A common feature of the schemes developed for both classes of these problems is that they are equivalent to box schemes (Keller [5]) and may be solved by the algebraic methods described by Keller in [6] (c.f. [2], [4], [8]). Such compact schemes for mixed initial boundary value problems avoid boundary extrapolation techniques which are generally required to make noncompact schemes algebraically determined and which can be an important source of errors.

The following notation will be employed:

$$(3) \quad \begin{aligned} \delta_x u_i^n &= (u_{i+\frac{1}{2}}^n - u_{i-\frac{1}{2}}^n) / \Delta x, & \delta_t u_i^n &= (u_i^{n+\frac{1}{2}} - u_i^{n-\frac{1}{2}}) / \Delta t, \\ \mu_x u_i^n &= (u_{i+\frac{1}{2}}^n + u_{i-\frac{1}{2}}^n) / 2, & \mu_t u_i^n &= (u_i^{n+\frac{1}{2}} + u_i^{n-\frac{1}{2}}) / 2. \end{aligned}$$

Clearly,

$$\delta(uv) = \mu(u)\delta(v) + \mu(v)\delta(u)$$

so that

$$\frac{1}{2}\delta(u^2) = \mu(u)\delta(u).$$

I. The Hyperbolic Problem

I.1 A Non-Dissipative Scheme.

In order to make this paper self-contained as well as to motivate the extension to be described below this section reviews a treatment of the system $U_t + AU_x = 0$ when A is symmetric and constant which has been given elsewhere (Rose [11]; also see Wendroff [12], [13]).

Consider the scheme

$$(I.1) \quad \begin{aligned} (a) \quad & \delta_t U_i^n + A \delta_x U_i^n = 0 \\ (b) \quad & \mu_t U_i^n = \mu_x U_i^n. \end{aligned}$$

Under the conditions just indicated this scheme provides a convergent approximation to (1) as the following sketch of an "energy" argument shows: multiply (I.1a) by $\mu_t U_i^n$ and employ (I.1b) to obtain

$$\delta_t ((U_i^n)' U_i^n) + A \delta_x ((U_i^n)' U_i^n) = 0.$$

Summing on i , setting

$$\|U^n\|^2 = \sum_i (U_i^n)' U_i^n \Delta x,$$

and noting that the boundary conditions (1b) were assumed to be dissipative, there results

$$(I.2) \quad \|U^n\| \leq \|U^0\|.$$

This estimate implies that the solution of (I.1) converges to the solution of (1) for all values of the mesh ratio $\lambda = \Delta t / \Delta x$, $\Delta x \rightarrow 0$. A closer examination also shows that the scheme (I.1) is non-dissipative.

The solution of (I.1) may be obtained by one of the following methods:

(i) Two-Step Method

(a) Eliminate $U_i^{n+1/2}$ from (I.1) to obtain

$$(I.3) \quad R_+(\lambda)U_{i+1/2}^n + R_-(\lambda)U_{i-1/2}^n = U_i^{n-1/2},$$

where

$$R_{\pm}(\lambda) \equiv \frac{1}{2}(I \pm \lambda A).$$

The difference equations (I.3) present a two-point algebraic boundary value problem which is solvable (Keller [6]) under the boundary conditions described in (1) with the initial conditions given by $U_i^{n-1/2}$.

(b) with U_i^n so determined, explicitly solve (I.1a) or (I.1b) for $U_i^{n+1/2}$.

(ii) One-Step Method (Box Scheme A)

Instead of employing the explicit step (b) eliminate $U_i^{n-1/2}$ from (I.1) to obtain

$$(I.4) \quad R_-(\lambda)U_{i+1/2}^n + R_+(\lambda)U_{i-1/2}^n = U_i^{n+1/2}.$$

Next replace n by $n+1$ in (I.4) and then eliminate $U_i^{n+\frac{1}{2}}$ from (I.3) and (I.4) to obtain

$$(I.5) \quad LU_i^{n+\frac{1}{2}} \equiv R_+(\lambda)U_{i+\frac{1}{2}}^{n+1} + R_-(\lambda)U_{i-\frac{1}{2}}^{n+1} - R_-(\lambda)U_{i+\frac{1}{2}}^n - R_+(\lambda)U_{i-\frac{1}{2}}^n = 0.$$

This algebraic system is similar to (I.3) and is solvable for $U_i^{n+\frac{1}{2}}$ by the same method. Its relationship to a box scheme is evident from the fact that the values occurring in (I.5) are associated with the vertex points of a computational cell centered at $(i, n+\frac{1}{2})$. The implementation of this scheme involves first employing step (a) in (i).

(iii) One-Step Method (Box Scheme B)

Equation (I.1b) is identically satisfied by introducing new variables V such that

$$2U_{i+\frac{1}{2}}^n = V_{i+\frac{1}{2}}^{n+\frac{1}{2}} + V_{i+\frac{1}{2}}^{n-\frac{1}{2}},$$

and

$$2U_i^{n+\frac{1}{2}} = V_i^{n+1} + V_i^{n-1}.$$

Substitution in (I.1) then yields a box scheme for values centered at (i, n) . This form of the box scheme method is essentially that developed by Keller [5] and will not be discussed in further detail in this paper.

Considered separately from (i) the box scheme formulations tend to obscure the existence of the simple energy estimate (I.2). However, the box scheme formulation has advantages for the analysis of other questions. Thus, an expansion of the operator $LU_i^{n+\frac{1}{2}}$ immediately results in a truncation error estimate which is proportional to $(\Delta x)^2$ while an analysis of the amplification matrix in (I.5) also shows the scheme to be non-dissipative and, hence, will be of limited use in treating discontinuous solutions. The following section describes a simple modification of (I.1) which yields a dissipative system.

I.2 A Dissipative Scheme

Instead of (I.1) consider the scheme

$$(I.6) \quad \begin{aligned} (a) \quad & \delta_t U_i^n + A \delta_x U_i^n = 0 \\ (b) \quad & \mu_t U_i^n = \mu_x U_i^n + \sigma A \delta_x U_i^n, \end{aligned}$$

with $\sigma \geq 0$.

Assuming again that A is symmetric and constant, and suppressing indices, the energy expression resulting from (I.6) is now

$$0 = \frac{1}{2} \int \{ \delta_t (U'U) + A \delta_x (U'U) \} + \sigma \int (\delta_x AU)' (\delta_x AU),$$

so that

$$(I.7) \quad \| U^n \| \leq \| U^0 \|.$$

Clearly this system is dissipative, i.e., when $\sigma > 0$ the inequality in (I.7) holds unless U^n is constant.

Let

$$\epsilon = 2\sigma/\Delta x$$

and

$$(I.8) \quad \lambda^\pm = \lambda \pm \epsilon.$$

The following solution methods now result:

(i) Two-Step Method

$$(I.9) \quad \begin{aligned} a) \quad & R_+(\lambda^+) U_{i+\frac{1}{2}}^n + R_-(\lambda^+) U_{i-\frac{1}{2}}^n = U_i^{n-\frac{1}{2}} \\ b) \quad & \delta_t U_i^n + A \delta_x U_i^n = 0. \end{aligned}$$

(ii) One-Step Method

$$(I.10) \quad L_{\epsilon} U_i^{n+\frac{1}{2}} \equiv R_+(\lambda^+) U_{i+\frac{1}{2}}^{n+1} + R_-(\lambda^+) U_{i-\frac{1}{2}}^{n+1} - R_-(\lambda^-) U_{i+\frac{1}{2}}^n - R_+(\lambda^-) U_{i-\frac{1}{2}}^n = 0.$$

Thus (I.9) and (I.10) result from (I.3) and (I.4) by appropriately increasing or decreasing the parameter λ . If $W_i^n = U_i^n - U$, where U is the solution of the differential equation in (1), the estimate of truncation error using (I.10) is

$$(\Delta t)^{-1} L_{\epsilon} W_i^{n+\frac{1}{2}} = 2\sigma A^2 U_{xx} + O(\Delta x^2),$$

so that the parameter $\sigma = \epsilon \Delta x / 2$ gives rise to an artificial viscosity term proportional to U_{xx} .

I.3 Amplification and Phase Error

Consider the scalar equation $u_t + au_x = 0$ where $a > 0$. Initial data given by $u^0 = \exp(i\theta x)$ are transformed by (I.6) into $v = \rho \exp[i(\theta x - \psi)]$ while the differential equation carries u^0 into $v' = \exp[i\theta(x - a\Delta t)]$. Eq. (I.10) shows that

$$(I.11) \quad \rho^2 = \frac{1 + (a\lambda^-)^2}{1 + (a\lambda^+)^2} < 1,$$

while

$$(I.12) \quad \frac{1}{2}\psi = \arctan(a\lambda \tan(\theta/2)).$$

Thus $|\rho| < 1$ for $\epsilon > 0$, i.e. (I.6) is dissipative for $\sigma > 0$.

For $a\lambda = 1$, $\psi = \theta$. Since $\tan \alpha \phi > \alpha \tan \phi$, $0 \leq \alpha < 1$, then $\psi < \theta$ for $0 < a\lambda < 1$; similarly $\psi > \theta$ for $a\lambda > 1$. Thus the wave velocity of

the wave solution of the differential equation according as the CFL number is the difference equation has the same relationship to that of less than, equal to, or greater than 1.

In the non-scalar case an analysis of the amplification matrix associated with (I.10) yields an inequality similar to (I.11). This observation also implies the convergence of the scheme (I.6) since it is, clearly, consistent with the differential equation (1).

I.4 Numerical Experiments

The preceding discussion concerned the case $A = \text{constant}$. For nonlinear problems, $A = A(U)$ and it is natural to apply (I.6) in which the coefficient A is determined by U^n . Because (I.6) is equivalent to an artificial viscosity method it may be expected that the dissipative scheme (I.6) will converge to the physical weak solution of the nonlinear conservation system $U_t + F_x(U) = 0$.

In one dimension the nonconservation form of the Euler equations for inviscid fluid flow is described by

$$U_t + AU_x = 0,$$

where $U = (\rho, u, p)'$ (ρ = density, u = velocity, p = pressure) and

$$(I.13) \quad A = \begin{pmatrix} u & \rho & 0 \\ 0 & u & \rho^{-1} \\ 0 & \gamma p & u \end{pmatrix}$$

($\gamma = 1.4$).

The results of several numerical experiments with Riemann problems employing the two-step method (I.9) will be presented here.

Figure 1 illustrates the numerical density profile of a shock travelling to the right with speed 0.979 which results from the initial conditions

$x < 0$	$x > 0$
$\rho = 0.313$	0.219
$u = 0.3$	0.0
$p = 0.166$	0.1

The indicated values of ρ and u on the left and p on the right were used to supply boundary conditions. The dissipation factor in (I.9) was $\epsilon = 0.15$ and $\Delta x = .01$. The value $\lambda = 1.04$ in Figure 1a approximates the situation in which the average value of the CFL numbers before and after the shock was 1. The smoothness of the transition across the shock and the fairly accurate tracking of the correct shock position (indicated by the vertical line) are evident. Figure 1b illustrates the result of increasing the CFL number on both sides of the shock ($\lambda = 1.3$) while in Figure 1c the average CFL number was reduced ($\lambda = 0.7$). The post shock oscillation when $\lambda = 1.3$ and the preshock oscillation when $\lambda = 0.7$ which was evident in the figures may be interpreted as the influence of the CFL number on the wave velocity as discussed in I.3.

Figure 2 illustrates the ρ , u , p profiles resulting from the initial conditions

$x < 0$	$x > 0$
$\rho = 1.0$	0.125
$u = 0.0$	0.0
$p = 1.0$	0.125

The analytical solution, represented in the figures by the continuous line, yields a shock with speed 1.822 and a contact with speed 0.878. The calculated values at time = 2.4 with $\Delta x = 0.1$, $\lambda = 0.6$, and a dissipation factor of $\epsilon = .125$ yielded results in fairly good agreement with the exact solution. The relative error of the shock speed was estimated to be 3% and the relative

error of the total energy was calculated to be 0.3%. The value $\lambda = 0.6$ chosen results in an average CFL number ≈ 1 through the shock zone. In this experiment the matrix A in (I.1) was estimated by

$$A_i^n = \frac{1}{2}[A(U_{i+\frac{1}{2}}^n)] + \frac{1}{2}[A(U_{i-\frac{1}{2}}^n)].$$

In both of the above experiments the dissipative factor ϵ was kept constant for all points.

II. Convective-Diffusion Equation

II.1 Difference Scheme

A motivation for this scheme will be given in the Appendix.

Consider the scalar convective-diffusion equation in the form described by (2a), i.e.

$$\begin{aligned} (II.1) \quad & u_t + au_x - vv_x = 0 \\ & u_x - v = 0. \end{aligned}$$

Let

$$\theta = a\Delta x/2v,$$

so that $|\theta|$ is the local cell Reynolds number.

Also let

$$\begin{aligned} (II.2) \quad & p(\theta) = \theta^{-2}(\theta \coth \theta - 1), \\ & q(\theta) = \theta p(\theta). \end{aligned}$$

The following approximations to p and q will be convenient:

$$\begin{aligned} (i) \quad & |\theta| < 3 : \quad p \sim 1/3, \quad q \sim \theta/3, \\ (ii) \quad & |\theta| \geq 3 : \quad p \sim |\theta|^{-1}, \quad q \sim \operatorname{sgn} \theta - 1/\theta. \end{aligned}$$

The proposed scheme for treating (II.1) is:

$$\begin{aligned}
 & \text{a) } \delta_t u_i^n + a \delta_x u_i^n - v \delta_x v_i^n = 0 \\
 & \text{b) } \mu_x u_i^n - \left(\frac{\Delta x}{2}\right)^2 p \delta_x v_i^n = \mu_t u_i^n \\
 & \text{c) } \delta_x u_i^n + \left(\frac{\Delta x}{2}\right) q \delta_x v_i^n = \mu_x v_i^n
 \end{aligned}
 \tag{II.3}$$

For convergence $\Delta x \rightarrow 0$ in which case the coefficients of p and q in (II.3) may be neglected. For $|\theta|$ large, however, the term involving p and q can provide important corrections to the scheme.

The difference equations (II.3) are clearly consistent with the differential equation (2). The convergence of the scheme for $\Delta x \rightarrow 0$ when $a = \text{constant}$, is most easily shown by employing the following "energy" argument: neglecting the terms in (II.3) which involve p and q and suppressing the indices (i,n) , multiply (II.3a) by $\mu_t u$ and then employ (II.3b,c) to obtain

$$0 = \frac{1}{2} \delta_t u^2 + \frac{1}{2} a \delta_x u^2 - v \delta_x (uv) + v (\delta_x u)^2.$$

Assuming the boundary conditions satisfy the dissipative inequalities related to (2) as described in the introduction, summation over the spatial index then yields

$$\|u^n\| \leq \|u^0\|, \tag{II.4}$$

where

$$\|u^n\| = \sum_i (u_i^n)^2 \cdot \Delta x.$$

(The inequality in (II.4) is strict unless u_i^n is constant). This implies the convergence of solutions of (II.3) to the solution of (2) as $\Delta x \rightarrow 0$ for all values of the ratio $\lambda = \Delta t / \Delta x$.

II.2 Solution Methods

The solution method described earlier for hyperbolic systems has a direct extension to the equations (II.3). It will be convenient to introduce the vector $W = (u, v)^T$ and the matrices

$$R_{\pm} = \frac{1}{2} \begin{bmatrix} (1 \pm a\lambda) & \mp (v\lambda + \frac{\Delta x}{2} p) \\ \pm 1 & -\frac{\Delta x}{2} (1 \mp q) \end{bmatrix}$$

and

$$S_{\pm} = \frac{1}{2} \begin{bmatrix} (1 \mp a\lambda) & \pm (v\lambda - \frac{\Delta x}{2} p) \\ \pm 1 & -\frac{\Delta x}{2} (1 \mp q) \end{bmatrix}.$$

The following solution methods result:

(i) Two-Step Method

By eliminating the term $u_i^{n+\frac{1}{2}}$ in (II.3a,b) there results

$$(II.6) \quad R_+ W_{i+\frac{1}{2}}^n + R_- W_{i-\frac{1}{2}}^n = \begin{pmatrix} u_i^{n-\frac{1}{2}} \\ 0 \end{pmatrix}.$$

This is an algebraic two-point boundary value problem which is solvable under the boundary conditions (2b) and the initial values $u_i^{n-\frac{1}{2}}$. With W_i^n determined, $u_i^{n+\frac{1}{2}}$ may be obtained explicitly from (II.3).

(ii) One-Step Method (Box-Scheme)

By eliminating the term $u_i^{n-\frac{1}{2}}$ in equations (II.3a) and (II.3b) and then relabeling the index n the following box scheme results:

$$(II.7) \quad LW_1^{n+1} \approx (R_{+1+\frac{1}{2}}^{n+1} + R_{-1-\frac{1}{2}}^{n+1}) - (S_{+1+\frac{1}{2}}^n + S_{-1-\frac{1}{2}}^n) = 0.$$

The truncation error, as estimated from this expression, is $O(\Delta x^2)$ for all values of the local cell Reynolds number $|\theta|$.

II.3 Numerical Results

The solution $u = \cos(x-t)\exp(-vt)$ of $u_t + u_x = \nu u_{xx} = 0$ was computed at $t = 4\pi$ using II.3 for $\nu = 10^{-2}$ and the values $\Delta x = \pi/20, \pi/40, \pi/80$. The L_1 norm of the numerical errors as a function of $\lambda = \Delta t/\Delta x$ are given in the following table:

Δx	$\lambda = 0.5$	$\lambda = 1.0$	$\lambda = 2.0$
$\pi/20$	1.7×10^{-3}	0.5×10^{-3}	9.3×10^{-3}
$\pi/40$	0.3×10^{-3}	0.27×10^{-3}	2.5×10^{-3}
$\pi/80$	0.8×10^{-4}	0.07×10^{-3}	0.6×10^{-3}

The results confirm the assertion made earlier that II.3 is second order accurate. Similar results were obtained using the L_2 norm.

Figure 3 indicates steady-state boundary layer profiles ($t=10$) for $u_t + au_x - \nu u_{xx} = 0$ with boundary conditions $u(0) = 1, u(1) = 0$ and initial condition $u(x,0) = (1-x)$; (II.3) was employed with $\Delta x = 1/20$ and $\lambda = 1$. The exact solution is indicated by the solid curves. The numerical results indicate fairly close agreement with the exact solution in the neighborhood of $x = 1$.

Figure 4 describes results for Burger's equation $u_t + (u^2/2)x = \nu u_{xx}$ with $u(x,0) = 1$ for $x < 0.5$ and $u(x,0) = 0$ for $x > 0.5$ for $\nu = 10^{-2}, 10^{-3}$ at time $t = 1.0$ using (II.3) with $\Delta x = 1/50$ and $\lambda = 1.0$; the vertical line indicates the position of the shock for the limiting value $\nu = 0$.

Figure 5 illustrates the solution of Burger's equation at time $t = 2.0$ (steady-state) with boundary condition $u(0) = 1$, $u(1) = -1$ and initial condition $u(x,0) = 1 - 2x$. The maximum value of the local cell Reynolds number was $R_c = 112.23$.

Appendix A

The Underlying Approximation Method

The schemes described in this paper have their origin in a common approximation method.

Divide the fundamental solution domain \mathcal{D} $0 < x < 1$, $0 < t < T$ uniformly into $M \cdot N$ rectangular cells each of area $\Delta x \Delta t$. If π_i^n is a typical cell with center point (x_i, t_n) let $\sigma_{i+\frac{1}{2}}^n$, $\tau_i^{n+\frac{1}{2}}$ denote its vertical and horizontal sides as indicated in Figure 6.

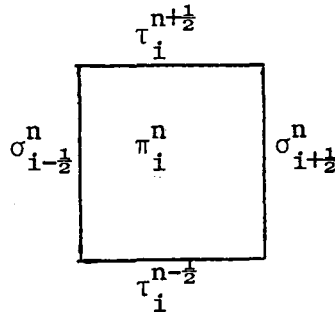


Figure 6

There are thus a total of $(M+1)N + (N+1)M$ sides of which $2(M+N)$ lie on the boundary of \mathcal{D} and $2MN - (M+N)$ lie interior to \mathcal{D} .

Consider first the equation $U_t + AU_x = 0$. If $U_i^{n+\frac{1}{2}}$ are the average values of U on the sides $\tau_i^{n+\frac{1}{2}}$, $\sigma_{i+\frac{1}{2}}^n$ of π_i^n then the MN conditions

$$(A.1) \quad \delta_t U_i^n + A \delta_x U_i^n = 0,$$

will imply that Gauss' theorem holds on the union of any contiguous set of cells. Suppose now that the global solution is approximated by functions which are solutions of the linear differential equation in each cell each of which depends, say, upon α parameters, i.e., if $\phi_1, \phi_2, \dots, \phi_\alpha$ are linearly independent solutions in a cell, we let

$$(A.2) \quad U \approx \sum_{i=1}^{\alpha} \phi_i c_i.$$

If $\alpha = 2$ the mixed initial-boundary value problem (1) may be approximated as follows (c.f. [10]): set $\phi_1 = I$, $\phi_2 = (xI - tA)$; then the parameters c_1, c_2 will be determined by any two of the four average values $U_i^{n+\frac{1}{2}}$ and $U_{i+\frac{1}{2}}^n$ associated with the sides of π_1^n . Elimination of the parameters yields two relationships between these values one of which is expressed by (A.1) and the other by

$$(A.3) \quad \mu_t U_i^n = \mu_x U_i^n.$$

There thus result $2MN$ conditions for the $2MN + (M+N)$ average values. By imposing the boundary and initial conditions in (1) a determined system of equations results. As we have shown through the use of an energy argument, when A is symmetric and constant this approximation method converges in an L_2 norm for smooth solutions. The numerical results presented earlier indicate that the dissipative scheme based upon a modification of this method provides accurate approximations to nonlinear problems as well.

For the scalar equation $u_t + au_x - vu_{xx} = 0$ similar arguments show that, if $v = u_x$, then

$$(A.4) \quad \delta_t u_i^n + a \delta_x u_i^n - v \delta_x v_i^n = 0,$$

is a necessary condition that Gauss' theorem hold in terms of the boundary data of cells. Employing (A.3) with $\alpha = 3$ and the elementary solutions

$$(A.5) \quad \begin{aligned} \phi_1 &= 1 \\ \phi_2 &= (x - at) \\ \phi_3 &= e^{ax/v} \end{aligned}$$

an elimination of parameters yields the scheme (II.3) which is a determined algebraic system under the initial-boundary values given by (2b). Again, the energy argument given earlier establishes the convergence of this approximation scheme when a is constant.

Both schemes employ an approximation basis which consists of wave solutions of the form

$$\phi(\beta, \gamma) = \exp[\beta(x - \gamma t)],$$

where γ is the wave velocity. In the hyperbolic case $\gamma = A$ and the polynomial basis $(1, xI - tA)$ results by setting $\phi_1 = \phi(0, A)$, $\phi_2 = \phi_\beta(0, A)$.

For the convective-diffusion equation the dispersion relationship $\gamma = a - v\beta$ holds. In addition to the polynomial solutions $(1, x - at)$ the function $\exp(ax/v)$ provides another linearly independent solution for which $\gamma = 0$ when $\beta = a/v$. The basis $(1, \exp(ax/v))$ is composed of solutions of the steady-state equation $au_x - vu_{xx} = 0$ and the method described above can be used to directly provide a difference scheme for the time-independent problem. The result is described by the two equations (II.3a) and (II.3c) in which the term $\delta_t u_1^n$ is set equal to zero. This same basis can be used to construct a Green's function on each overlapping subinterval $[x_{i-1}, x_{i+1}]$ having its singularity at $x = x_i$, $x_{i-1} < x_i < x_{i+1}$, a technique which leads to a positive definite tridiagonal difference scheme for Sturm-Liouville problems as shown in [9]. An equivalent point of view has been independently developed and applied to similar singular perturbation problems which arise from steady-state problems (for example, c.f. [1], [3], [7], [10]). In this sense the methods described in this paper appear to provide the appropriate extension of such Green's function techniques to time-dependent problems.

For the convective-diffusion equation a polynomial approximation basis also results by taking

$$\phi_1 = \phi(0,a) = 1$$

$$\phi_2 = \phi_\beta(0,a) = x - at$$

$$\phi_3 = \frac{1}{2} \phi_{\beta\beta}(0,a) = \frac{1}{2}(x-at)^2 + \nu t.$$

The difference scheme which is the consequence may be obtained from (II.3) by setting $p = q = 0$. In view of earlier remarks this basis can be expected to provide an accurate approximation only when the cell Reynolds number $|\theta|$ is small.

Concluding Remarks

This paper has described related implicit difference schemes for treating hyperbolic systems of equations and the scalar convective diffusion equation both of which share a common approximation rationale as well as a common solution technique. Numerical evidence indicates that both schemes can be employed to treat nonlinear problems. The accuracy of approximation to the dissipative hyperbolic problem is proportional to an artificial diffusion parameter σ while the approximation to the convective-diffusion is second order accurate and is independent of the value of the local cell Reynolds number. For both schemes conventional energy estimates are available when the coefficients are constant.

One important limitation of this study is its restriction to one dimensional problems; in another paper we will indicate how multi-dimensional problems may also be treated.

Acknowledgment

We wish to thank S. Wornom for valuable assistance with early numerical experiments and to V. Pereyra and J. Flaherty for helpful assistance about numerical methods underlying the solution of algebraic two-point boundary value problems.

References

- [1] A. E. Berger, J. M. Solomon, and M. Ciment, *Uniformly accurate difference methods for a singular perturbation problem*, Proc. Intl. Conference on Boundary and Interior Layers, Computational and Asymptotic Methods, J. J. H. Miller, ed., Boole Press, Dublin, 1980, pp. 14-28.
- [2] C. deBoor and R. Weiss, *Solveblok: A package for solving almost block diagonal linear systems, with applications to spline approximation and numerical solution of ordinary differential equations*, MRC Technical Report No. 16-75, University of Wisconsin Press, Madison, WI.
- [3] T. M. El-Mistikawy and M. J. Werle, *Numerical method for boundary layer with blowing-the exponential box scheme*, AIAA J., Vol. 16, 1978, pp. 749-751.
- [4] J. E. Flaherty and W. Mathon, *Collocation with polynomial and tension splines for singularly perturbed boundary value problems*, SIAM J. on Sci. and Stat. Computing, Vol. 1, No. 2, June 1980, pp. 260-289.
- [5] H. B. Keller, *Numerical methods in boundary layer theory*, Annual Rev. Fluid Mech., Vol. 10, 1978, pp. 417-433.
- [6] H. B. Keller, *Numerical solution of two point boundary value problems*, Regional Conference Series in Applied Mathematics, 24, SIAM, 1976.
- [7] A. M. Il'in, *Differencing scheme for a differential equation with a small parameter affecting the highest derivative*, Mat. Zametki, Vol. 6, 1969, pp. 237-248, Math. Notes, Vol. 6, pp. 596-602.

- [8] M. Lentini and V. Pereyra, *An adaptive finite difference solver for nonlinear two-point boundary problems with mild boundary layers*, SIAM J. Numer. Anal., Vol. 14, 1977, pp. 91-111.
- [9] M. E. Rose, *Finite difference schemes for differential equations*, Math. Comput., Vol. 18, No. 86, 1964, pp. 179-195.
- [10] M. E. Rose, *Weak element approximation to elliptic differential equations*, Numer. Math., Vol. 24, 1975, pp. 185-204.
- [11] M. E. Rose, *A treatment of the wave equation and the Cauchy-Riemann equations*, to appear in SIAM J. Numer. Anal.
- [12] B. Wendroff, *On centered difference equations for hyperbolic systems*, J. Soc. Indust. Appl. Math., Vol. 8, No. 3, 1960, pp. 549-555.
- [13] B. Wendroff, *The structure of certain finite difference schemes*, SIAM Review, Vol. 3, No. 3, 1961, pp. 237-242.

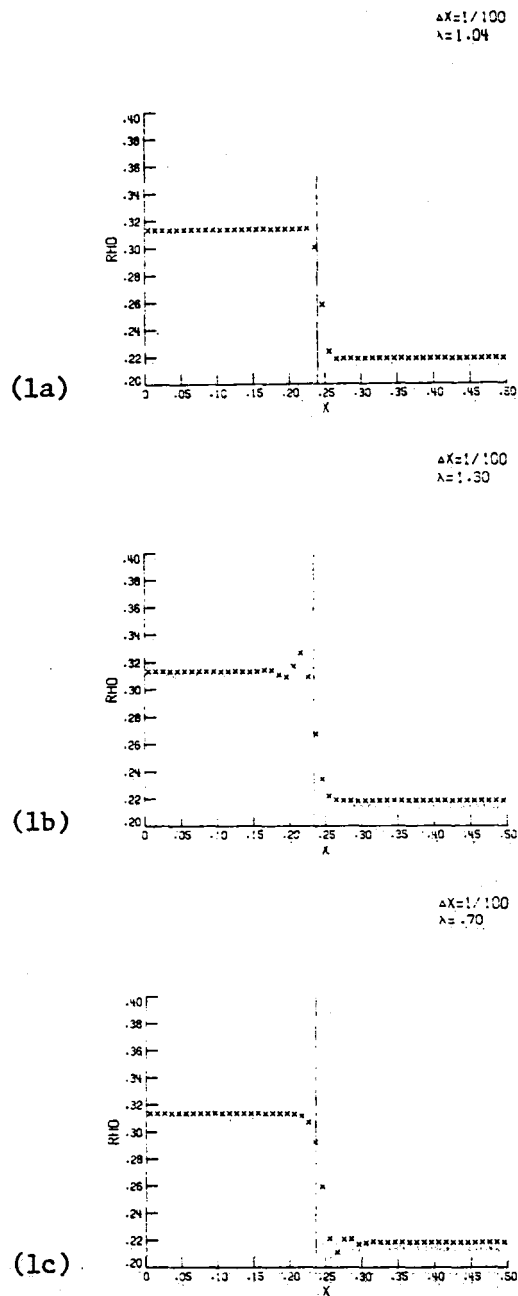


Figure 1. Density profile of a shock calculation showing the influence of the CFL number upon pre- and post- oscillations (Scheme I.6).

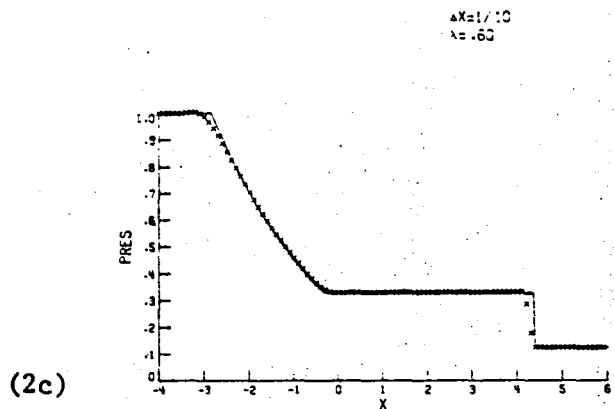
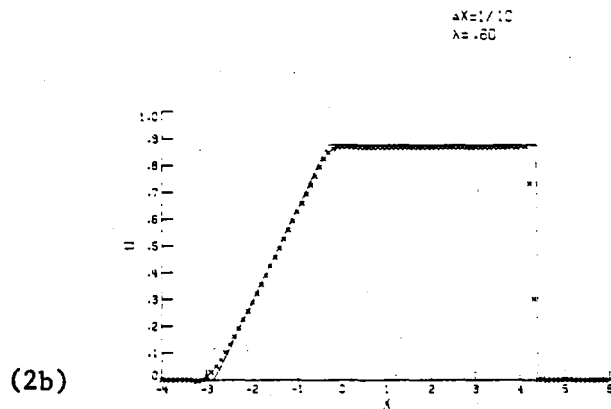
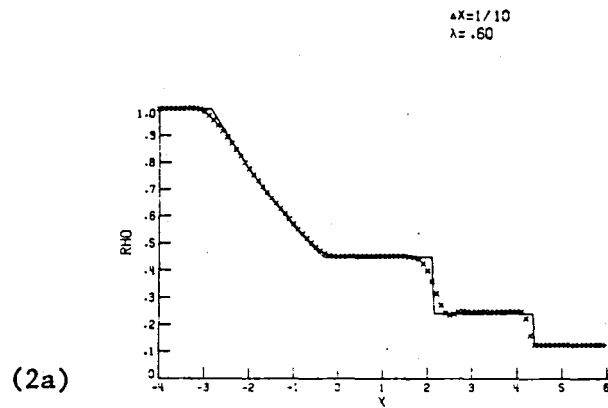


Figure 2. A comparison of the numerical and exact solution of a Riemann problem; the shock speed exhibits a relative error of 3% (Scheme I.6).

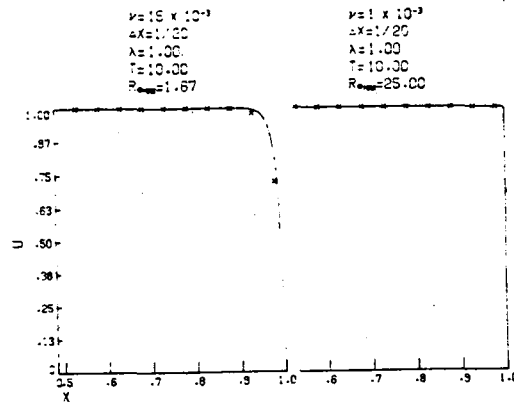


Figure 3. A comparison of boundary layer profiles for various cell Reynolds numbers.

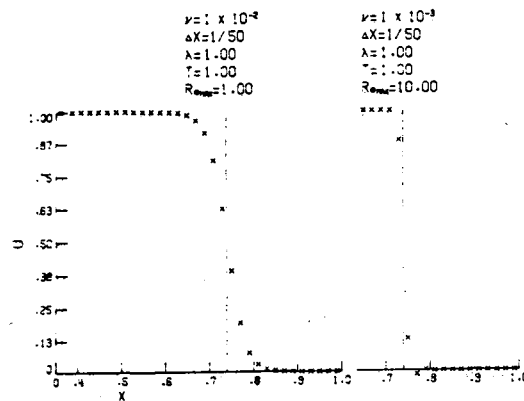


Figure 4. Solutions of Burger's equation for different viscosity values.

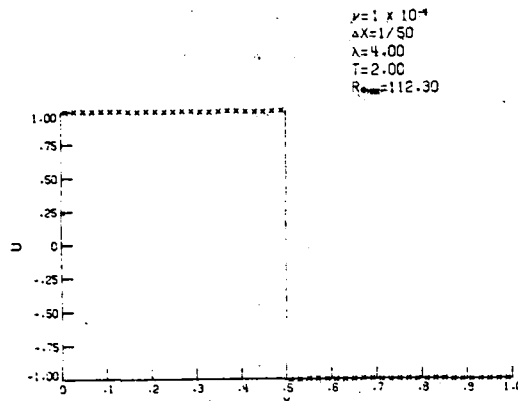


Figure 5. Steady-state solution of Burger's equation.

End of Document